



Lithium niobate/lithium tantalate single-crystal thin films for post-moore era chip applications

Yixin Zhu^{1,2} · Qing Wan^{1,3}

Received: 2 November 2023 / Revised: 22 January 2024 / Accepted: 31 January 2024
© The Author(s) 2024

Abstract

Lithium niobate (LiNbO_3) and lithium tantalate (LiTaO_3) are a class of multifunctional materials with excellent piezoelectric/ferroelectric, electro-optic, and nonlinear optical properties, which have wide applications in high-performance radio frequency filters, optical communications, integrated photonics, quantum information, and other fields. With the advent of the post-Moore era of integrated circuit technology, $\text{LiNbO}_3/\text{LiTaO}_3$ thin-film also shows great potential and advantages in new concept chip applications. High-quality single-crystal thin films lay the foundation for high-performance radio frequency, optoelectronic, and quantum devices and their integration. This review first introduces the main characteristics of $\text{LiNbO}_3/\text{LiTaO}_3$ single-crystal thin films, such as ferroelectricity, piezoelectricity, electro-optic effect and nonlinear optical effect, then introduces the preparation methods of $\text{LiNbO}_3/\text{LiTaO}_3$ single-crystal thin films represented by smart-cut and their application progress in different fields such as waveguides, modulators, laterally excited bulk acoustic wave resonators, and quantum devices. The application prospects and challenges of $\text{LiNbO}_3/\text{LiTaO}_3$ single-crystal thin films in post-Moore era chips are also discussed in this article, aiming to provide valuable references for their development and application.

Keywords $\text{LiNbO}_3/\text{LiTaO}_3$ · Thin films · Smart-cut · Radio frequency filters · Integrated photonics · Post-Moore era

1 Introduction

Lithium niobate (LiNbO_3 , LN) and lithium tantalate (LiTaO_3 , LT), distinguished by their exceptional performance and wide-ranging applications, have engendered substantial research interest in recent years [1, 2]. From facilitating high-speed optical communication, which forms the foundation of the internet, to their utilization in radio-frequency (RF) filtering within mobile devices, and from classical integrated optics to the realm of quantum optics, these versatile materials have profoundly reshaped our daily existence [3]. The successful production of 8-inch wafers, the synthesis of high-quality single-crystal thin films, and

the evolution of processing methodologies have ushered in unparalleled prospects for the domains of optical communication and integrated photonics. The advent of the “Lithium Niobate Era” looms on the horizon.

LN and LT are endowed with exceptional optical properties, including high refractive indices, low optical losses, broad spectral bandwidths, and high nonlinear coefficients. These attributes endow them with the capacity to facilitate a wide array of intricate optical functionalities, encompassing waveguides, resonant cavities, modulators, and filters [3–6]. Despite the decades of development, conventional LN/LT devices, such as bulk LN waveguides, have found practical utility in high-speed modulators, telecommunications waveguide amplifiers, and quantum light sources, among other applications. However, the restricted refractive index contrast inherent in bulk LN has significantly limited the potential for devices founded upon this material. The emergence of LN/LT single-crystal thin films has transformed this landscape. Almost concurrently, in 2001, Wan et al. and the French company SOITECH introduced the concept of utilizing the smart-cut process to transfer $\text{LiNbO}_3/\text{LiTaO}_3$ single-crystal thin films [7, 8]. In essence, this thin-film technology, initially developed for silicon-on-insulator

✉ Qing Wan
qing-wan@ylab.ac.cn

¹ Yongjiang Laboratory, Ningbo 315201, China

² School of Electronic Science and Engineering, and Collaborative Innovation Center of Advanced Microstructures, Nanjing University, Nanjing 210023, China

³ School of Micro-Nano Electronics, Hangzhou Global Scientific and Technological Innovation Centre, Zhejiang University, Hangzhou 310027, China

(SOI) applications, enables the controlled transfer of any crystalline material to an insulating substrate, while preserving its original crystallographic attributes. The application of this technology to LN/LT single-crystal thin films has permitted photonic devices or circuits to scale down to sub-micrometer dimensions, all the while retaining the exceptional properties of bulk materials. This advancement has directly propelled the rapid evolution of photonics. Capitalizing on strides in the preparation and processing techniques for high-quality single-crystal thin films, high-performance devices grounded in LN/LT have flourished in recent years, as illustrated in Fig. 1. LN/LT single-crystal thin films are poised to emerge as the material of preference for realizing classical and quantum applications in the post-Moore era.

This review aims to elucidate the applications of LN/LT single-crystal thin films in the post-Moore era. The initial section offers an introduction to the distinctive attributes of these materials. The subsequent section delves into the methodologies for preparing and processing single-crystal thin films. Sections three through six expound upon the applications of LN/LT single-crystal thin films in waveguides, electro-optic modulators, resonators/filters, and quantum technologies, respectively. Lastly, we address the challenges and opportunities in the evolution of LN-based

devices. We hope that this review will furnish valuable insights and inspiration for researchers seeking to explore the chip applications of LN/LT thin films in the post-Moore era.

1.1 Material characteristic

Due to their performance and structural similarity, LN will be employed as an illustrative case to introduce the material's characteristics and the fabrication of thin films. While LN crystals are not naturally occurring, the availability and abundance of crystalline materials facilitate the production of high-quality, sizable single crystals. LN crystal is noteworthy for its possession of the highest Curie temperature, standing at 1210 °C, outstripping other ferroelectric materials, including LT (610 °C). This exceptional Curie temperature secures the enduring stability of its ferroelectric phase, rendering it amenable to specific manufacturing procedures. Various pivotal characteristics of LN have been compared with other materials commonly employed in integrated photonics, as detailed in Table 1 [3]. The noteworthy second and third-order nonlinear coefficients of LN find widespread applications in processes such as second harmonic generation (SHG) [9, 10], photon pair generation

Fig. 1 Overview of LN/LT photonics

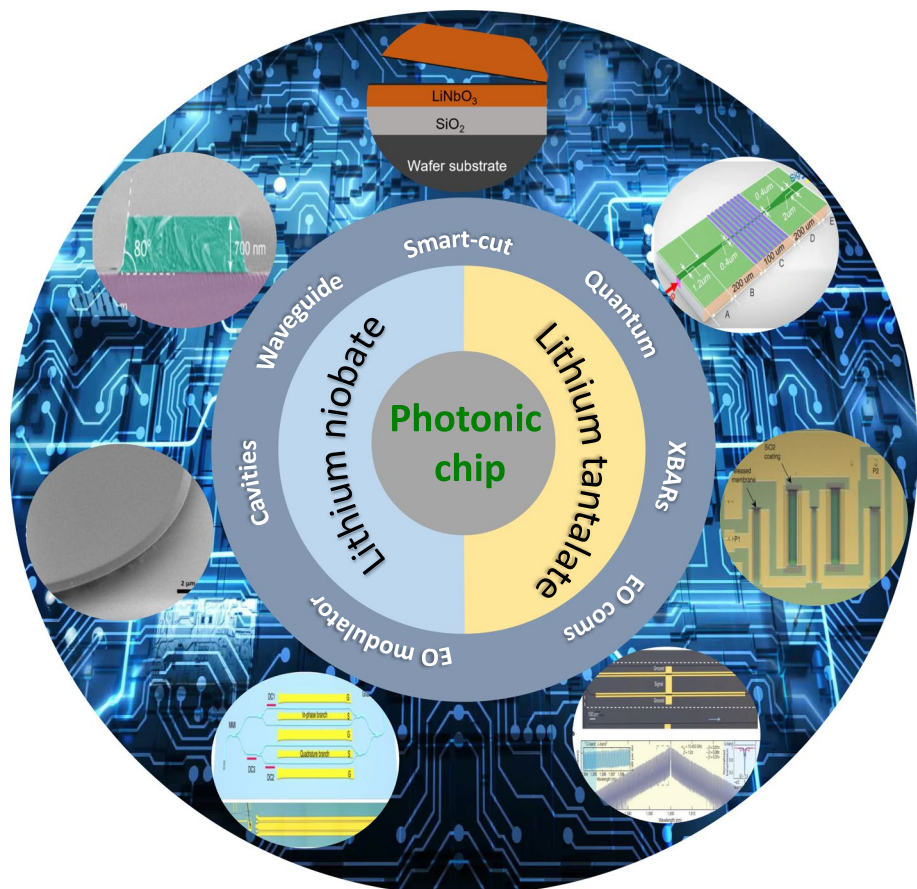


Table 1 Comparison of key characteristics of commonly used materials in integrated photonics

Material	LN	LT	Si	SiO ₂	Si ₃ N ₄	GaAs
EO Coefficient(pm/V)	9.6 (r_{13}) 6.8(r_{22}) 30.9(r_{33}) 32.6(r_{51})	8.4(r_{13}) −0.2(r_{22}) 30.5(r_{33}) 20(r_{51})	0	0	0	1.4 (r_{41} ,1550 nm)
Optical Refractive Indices (1550 nm)	2.2(o) 2.1(e)	2.1(o) 2.1(e)	3.5	1.4	2.0	3.4
Photoelastic Coefficients	−0.026(p_{11}) 0.09(p_{12}) 0.133(p_{13}) −0.075(p_{14}) 0.179(p_{31}) 0.071(p_{33}) −0.151(p_{41}) 0.146(p_{44})	−0.081(p_{11})0.081(p_{12}) 0.093(p_{13}) −0.026(p_{14}) 0.089(p_{31}) −0.044(p_{33}) −0.085(p_{41}) 0.027(p_{44})	−0.094(p_{11}) 0.017(p_{12}) 0.051(p_{44})	0.121(p_{11}) 0.270(p_{12})	0.047(p_{12})	−0.165(p_{11}) −0.140(p_{12}) −0.072(p_{44})
RF Dielectric Constant	44.0($\epsilon_{11,22}$) 27.9(ϵ_{33})	38.3($\epsilon_{11,22}$) 46.2(ϵ_{33})	11.7	3.9	7.5	12.9
Piezoelectric Strain Coefficient (pC/N)	−1.0(d_{31}) 21(d_{22}) 16(d_{33}) 74(d_{15})	−3.0(d_{31}) 9.0(d_{22}) 9.0(d_{33}) 26(d_{15})	0	0	0	2.6(d_{14})
Second-Order Nonlinear Coefficient (pm/V) (1064 nm)	−4.3(d_{31}) −27.0(d_{33}) 2.1(d_{22})	0.85(d_{31}) 13.8(d_{33})	0	0	0	170(d_{36})
Nonlinear Refractive Indices (m ² /W)	1.8 × 10 ^{−19} 1550 nm	1.5 × 10 ^{−19} 800 nm	5.0 × 10 ^{−18} 1550 nm	3.0 × 10 ^{−20} 1550 nm	2.5 × 10 ^{−19} 1550 nm	2.6 × 10 ^{−17}

[11, 12], and frequency comb generation [13]. Furthermore, its exceptional electro-optic (EO) effect designates it as the favored material for EO modulators. LN boasts a wide transparent spectral window encompassing visible to mid-infrared wavelengths. Within the visible spectrum, applications like frequency conversion and quantum communication/computing can be realized on the LN platform [4, 14]. At around 1550 nm, LN has been extensively employed for optical modulation in telecommunications [15, 16]. In the higher infrared wavelengths, certain nonlinear optical conversions and additional applications can also be accomplished utilizing LN. In the field of acoustics, LN exhibits a higher acoustic index compared to SiO₂. Its notable piezoelectric coefficient and outstanding photoelastic coefficient position it with significant application prospects in surface acoustic wave (SAW) filters and laterally-excited bulk-wave resonators (XBARs) devices, among other front-end radio-frequency applications.

1.2 LN/LT thin film

While conventional devices relying on bulk LN have garnered substantial attention and utilization in RF signal processing, the restricted refractive index contrast has imposed significant limitations on the advancement of bulk lithium niobate devices. This encompasses the realization of closely confined waveguides and low-loss resonators. Furthermore, the increasing need for on-chip integration has spurred the pursuit of thin-film LN crystals. Prior

to the introduction of the smart-cut process, there were initial endeavors to investigate the fabrication of high-quality lithium niobate single-crystal thin films [17–21]. Despite the exploration of various fabrication methods, the attainment of satisfactory high-quality single-crystal thin films remained an elusive objective.

The smart-cut technique also recognized as crystal ion slicing, originally devised for the manufacture of silicon wafers on insulating substrates, has evolved into the prevailing technology for the commercial production of LN single-crystal thin films. The application of this methodology to LN and LT materials traces its origins back to the early twenty-first century. Levy et al. were pioneers in this endeavor, as they first reported the utilization of high-energy helium ions (3.8 MeV) vertically introduced into LN crystals, succeeded by etching with hydrofluoric acid [22]. This process yielded LN single-crystal thin films with an approximate thickness of 9 μm. In 2001, Wan et al. and the French company SOI Tech almost concurrently disclosed the technique of smart-cut to achieve the detachment and transfer of LN/LT single-crystal thin films [7, 8]. This pivotal development marked the commencement of the commercialization of LN/LT single-crystal thin films. Subsequently, in 2009, Hu et al. accomplished the bonding of 3-inch LN single-crystal thin films onto SiO₂ substrates, leading to the creation of LN on insulator (LNOI) [23]. Presently, NanoLN company has achieved the successful commercialization of 3 to 6-inch LN/LT thin films.

1.2.1 Smart-cut

Figure 2 provides a schematic representation of the smart-cut process employed for the production of LN single-crystal thin films. Broadly, this process entails three fundamental stages: ion implantation, wafer bonding, and chemical mechanical polishing (CMP). In the smart-cut process for fabricating LN single-crystal thin films, He^+ with energies ranging from 200 to 400 keV are precisely implanted into the surface of a LN wafer grown using the Czochralski method. When He^+ with uniform energy levels are implanted into the crystal under the influence of an electric field, they perturb the crystal structure in their vicinity, creating a damaged layer. Given the uniformity of ion implantation energy, this interface effectively segregates the wafer into upper and lower layers. The dimensions of the initial wafer dictate the ultimate size of the resulting single-crystal thin film. It is imperative to emphasize that maintaining the original optical properties of bulk LN is of utmost importance, necessitating that the LN thin film remains single-crystalline. Nevertheless, during the ion implantation process, He^+ infiltrate from the surface into the crystal, causing some degradation in the resulting thin film. Subsequent steps are mandated to rectify the damage and defects induced by ion implantation.

In the context of LNOI wafers, commonly employed substrates include SiO_2 and LN itself. The process entails depositing a SiO_2 layer, typically a few micrometers thick, onto another LN wafer, which serves as the substrate. This

deposition can be achieved through methods such as thermal oxidation or plasma-enhanced chemical vapor deposition. Subsequently, the surface is meticulously polished until it attains a smooth and flat finish using CMP in preparation for the subsequent bonding process.

In the wafer bonding process, the ion-implanted LN wafer is inverted and bonded to the substrate. When manufacturing at the wafer level, the pre-bonded surfaces are sufficiently smooth and have a small total thickness variation to facilitate direct bonding. This approach also allows for higher annealing temperatures, which are instrumental in rectifying lattice damage stemming from ion implantation. Moreover, benzocyclobutene (BCB) can serve as an intermediary bonding material. BCB bonding is advantageous as it has less stringent flatness requirements for the bonding surface and is an active area of research. However, it is important to note that LNOI can also be produced using BCB [24, 25]. Nevertheless, it may exhibit stability issues, particularly when subjected to high-temperature processing. As a result, direct bonding is the preferred approach for wafer production, while BCB is more commonly employed in research applications.

High-temperature heating serves to bolster the bonding strength between the LN and the contact surfaces of the substrate. Subsequent to bonding, a crucial step in the process involves thermal annealing, which is employed along the damaged layer to facilitate the separation of the substrate, ultimately leading to the transfer of the LN thin

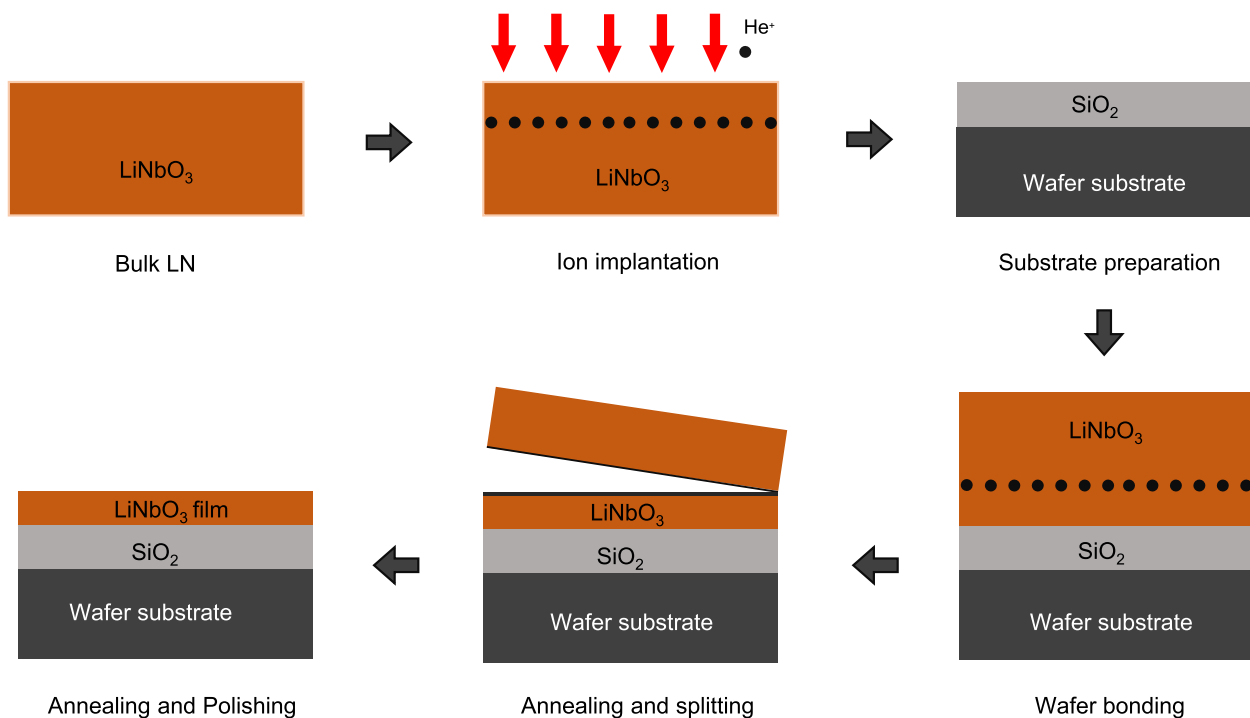
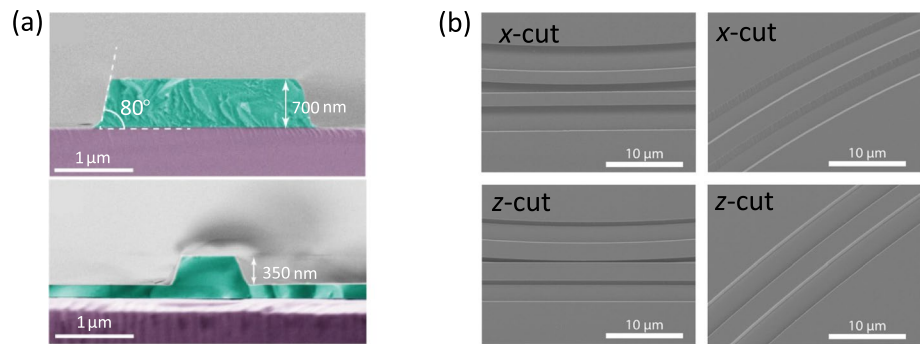


Fig. 2 Smart-cut process steps

Fig. 3 **a** Scanning electron microscope (SEM) images of etched optical waveguide. Reprinted by permission from [27] Copyright © 2023, Springer Nature Limited. **b** SEM images of x-cut and z-cut LN structures after wet etching. Reprinted by permission from [30] © 2022 Wiley-VCH GmbH



film. Significantly, moderate high-temperature annealing, typically in the range of 150–250 °C, induces the damaged layer to form bubbles, allowing for the easy detachment of the LN thin film from the parent LN crystal. Furthermore, additional high-temperature annealing steps, typically carried out at temperatures ranging from 400–500 °C, are essential for minimizing damage to the LN thin film. This is pivotal in restoring the material's electro-optical properties and other intrinsic characteristics.

Post-annealing, LNOI wafers necessitate flattening due to the unevenness of the cleaved surface, which is accomplished through CMP. The ultimate thickness of the LN thin film is determined by both the energy of He⁺ implantation and the final CMP polishing process. This technology has already achieved wafer-scale production of LN/LT single-crystal thin films on SiO₂ substrates. Evidently, this approach can also be extended to produce other high-quality thin films. Presently, companies like NanoLN, shnsit, PAMxiamen, Partow Technology, SRICO, NGK Insulators, and others have successfully commercialized 4-inch or 6-inch LN/LT thin films.

1.2.2 Etching process

Dry etching is a fundamental process in modern silicon-based technology and optoelectronics. This causes the etching of LN to become a hindrance. In the context of LN thin films, dry etching plays a key role in fabricating high-precision micro-nanostructures. Notably, it is a non-contact process, which mitigates material contamination concerns. Presently, there are several primary dry etching methods for LN, including laser micromachining, reactive ion etching (RIE), inductively coupled plasma (ICP) etching, focused ion beam (FIB) etching, among others. Devices etched with Ar⁺ demonstrate flat surfaces and nearly vertical sidewalls [26]. The use of a hard mask (such as an electrolyte or metal) can further enhance the etching selectivity. Li et al. employed a hard mask composed of diamond-like carbon, thereby demonstrating deeply etched, low-loss waveguides, as depicted in Fig. 3a [27]. At present, ICP-RIE is still the

optimal etching method for LN, which can provide good control over the shape of LN in different tangential directions [28, 29].

Wet etching is an alternative technique for processing LN. In contrast to dry etching, wet etching offers cost-effectiveness and efficiency, making it a widely adopted method in various materials processing applications. When it comes to LN processing, dry etching may necessitate expensive etching equipment. Processing larger wafers, such as those measuring 4-inches or more, can be time-consuming, with only one wafer being processed at a time. Conversely, wet etching is capable of handling multiple wafers simultaneously under similar conditions, devoid of size constraints. Li et al. illustrated the processing of LN thin film wafers using wet etching, yielding etching results comparable to those achieved through dry etching, as displayed in Fig. 3b [30]. Still, wet etching makes it difficult to create sufficiently steep sidewalls, which is critical to subsequent device performance.

Another method for processing LN thin films entails direct grinding and polishing. After bonding bulk LN crystals to a substrate, the bulk LN can be thinned down to a few micrometers through continuous grinding and polishing. While this approach yields thicker films and larger device sizes in comparison to the smart-cut technique, it avoids ion implantation, thereby minimizing damage to the crystal structure.

1.3 Waveguide

Waveguides constitute pivotal components within the realm of integrated photonics. Traditional bulk LN waveguides are typically formed via techniques such as titanium diffusion or proton exchange [31]. These processes, however, result in a relatively lower refractive index contrast and subsequently lead to weaker light confinement. Such weak optical confinement can, in turn, adversely impact the performance of devices, particularly modulators. The advent of thin-film LN has ushered in a new era in the fields of integrated photonics and microwave photonics. Notably, LN itself presents

challenges in terms of etching, rendering the etching process a critical aspect of its various applications. Presently, both dry etching and wet etching processes are employed to pattern the material and create optical waveguides.

In comparison to their bulk counterparts, thin-film LN waveguides offer greater potential for achieving compact, low-loss waveguide bends and diverse micro resonator shapes, which can be challenging to realize in bulk LN. The typical process of fabricating ridge waveguides via dry etching is illustrated in Fig. 4a. Initially, the desired waveguide pattern is delineated through photolithography, followed by the deposition of a thin metal film serving as an etch mask. Subsequently, the non-waveguide regions are cleared of the photoresist and Cr, and etching is executed. To ensure

a smooth waveguide surface and eliminate residues, post-etching steps like chemical etching or CMP are commonly employed. Peruzzo et al. achieved commendably low propagation losses of 0.4 dB/cm with ridge waveguides fabricated through dry etching, featuring a sidewall angle of 75° , as shown in Fig. 4b [32]. Notably, the roughness of the sidewalls significantly contributes to propagation losses, which can be mitigated effectively through sidewall polishing. As depicted in Fig. 4c, Wolf et al. further reduced propagation losses to 0.04 dB/cm through a combination of sidewall polishing and the use of a protective metal layer on the top surface [33]. Zhang et al. introduced an alternative approach by replacing the Cr etch mask with hydrogen silsesquioxane photoresist [34]. This substitution, coupled with meticulous

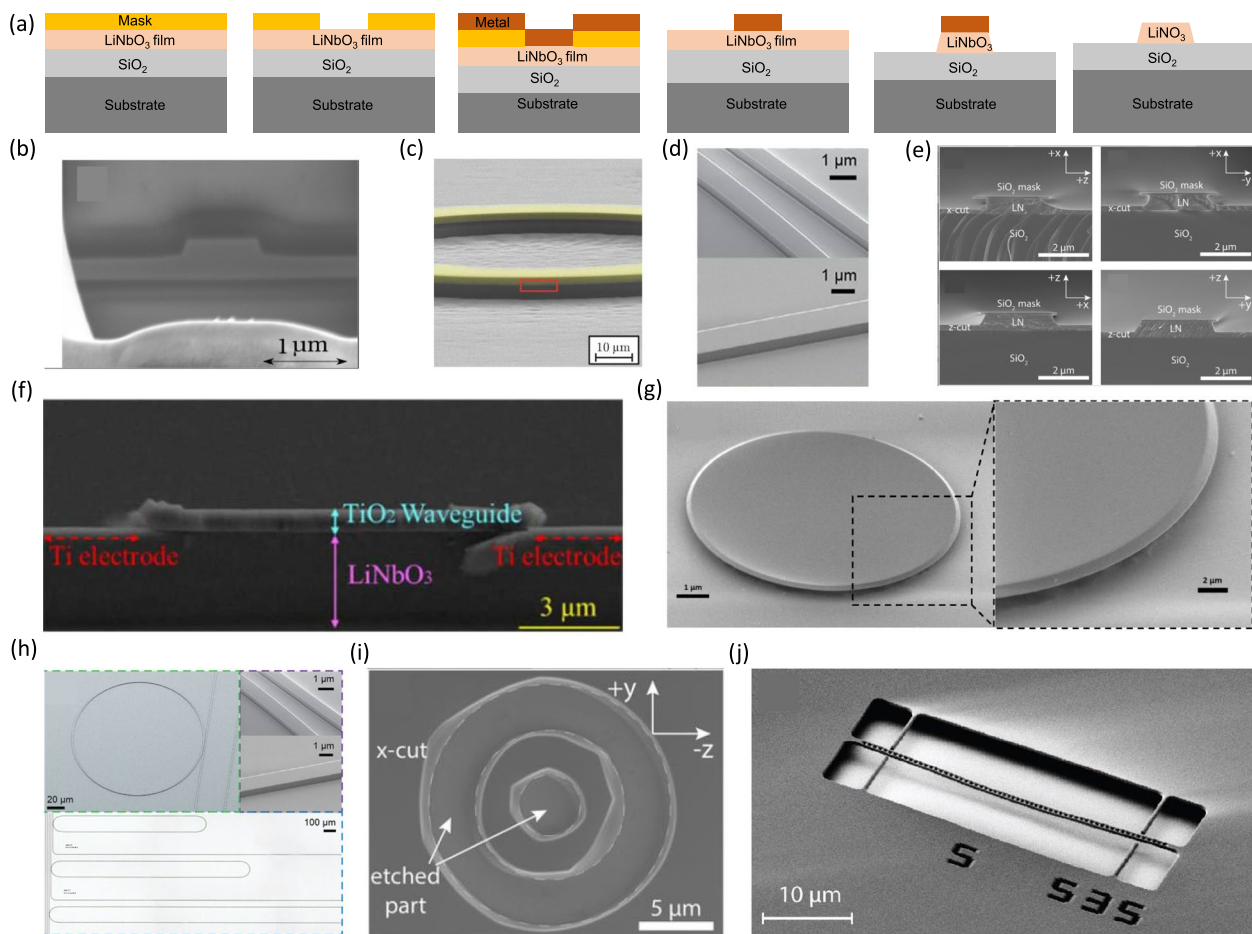


Fig. 4 **a** Process steps to fabricate LN waveguides using lithography (such as lithography or EBL) and dry etching methods. **b** The cross-sectional view of the device. Reprinted by permission from [32] © 2018 Optical Society of America. **c** SEM image of polished waveguides. Reprinted by permission from [33] © 2018 Optical Society of America. **d** Close-up of the etched waveguides. Reprinted by permission from [34] © 2017 Optical Society of America. **e** Ridged waveguide obtained by wet etching. Reprinted by permission from [30] © 2022 Wiley-VCH GmbH. **f** The cross-sectional view of the hybrid waveguide. Reprinted by permission from [38] Copyright ©

2019. **g** SEM image of a suspended LN microdisk supported by a silica pedestal on top of a LN substrate. Reprinted by permission from [39] © 2014 Optical Society of America. **h** SEM (top) and optical microscope (bottom) images of a microring and micro-racetrack resonators of various lengths. Reprinted by permission from [34] © 2017 Optical Society of America. **i** SEM images of wet etched microrings based on *x*-cut and *z*-cut LN. Reprinted by permission from [30] © 2022 Wiley-VCH GmbH. **j** SEM image of a fabricated LN photonic crystal cavity. Reprinted by permission from [40] © 2017 Optical Society of America

process control, yielded waveguides with propagation losses as low as 0.027 dB/cm, as depicted in Fig. 4d. More recently, Cheng et al. introduced a novel method known as CMPL, which combines the fine polishing of sidewalls with full-spectrum laser (femtosecond-laser) ablation for surface patterning [35]. Through this innovative approach, they successfully achieved an impressive reduction in propagation losses to 0.027 dB/cm, coupled with an exceptionally low surface roughness of merely 0.452 nm. Lu and colleagues employed femtosecond laser micromachining in conjunction with liquid-phase epitaxy to fabricate LN/LT ridge waveguides [36]. The LN waveguides exhibited propagation losses of 2.6 dB/cm and demonstrated SHG at 980 nm. Nishi and collaborators presented a LTOI waveguide, characterized by impressively low propagation losses of 0.28 dB/cm [37]. Furthermore, they successfully realized ring resonators with quality factors (Q-factors) exceeding 10^6 within this waveguide platform. It's worth noting that wet etching also stands as a viable method for etching lithium niobate waveguides, as demonstrated in Fig. 4e [30].

Rib-loaded waveguides represent an alternative waveguide configuration that eliminates the necessity for LN etching processes. In this approach, a layer of material such as TiO_2 [38], Si [41], SiN_x [42], and other suitable candidates is deposited onto unetched LN thin films, as depicted in Fig. 4f. This auxiliary material is more amenable to deposition and etching processes, allowing for the creation of rib waveguides atop the LN substrate. LN thin films can be seamlessly integrated with silicon photonics circuits on SOI substrates through bonding, giving rise to the creation of hybrid waveguides. This innovative approach not only addresses the inherent absence of second-order optical nonlinearity in silicon but also provides a pathway for the development of high-performance, complementary metal–oxide–semiconductor (CMOS)-compatible thin-film LN devices. There are two distinctive schemes for the realization of hybrid waveguides: one entails the direct bonding of LN thin films to existing silicon waveguides, while the other method combines etched LN waveguides with silicon waveguides in a heterogeneous fashion. Both of these approaches necessitate meticulous bonding processes and lithography techniques for the fabrication of the LN waveguides. In comparison to directly etched LN waveguides, hybrid waveguides hold the advantage of achieving higher effective refractive indices and exhibit enhanced potential for achieving compact waveguide bends. This versatility makes hybrid waveguides a compelling choice for integrated photonic circuits that seek to harness the benefits of LN thin films within the silicon photonics framework.

1.4 Optical microcavities

LN microresonators are typically produced using micro and nanofabrication techniques, which involve the creation of micro-scale optical structures designed to confine and guide light within them. Optical microresonators with exceptionally high-quality factors have gained widespread use in various applications, including EO modulators and nonlinear wavelength converters. Microdisk resonators, for instance, can effectively confine resonant light waves, facilitating the circulation of excited whispering gallery modes along their circumferences [43]. Microresonators boasting high Q-factors can trap light within a small volume for an extended period, making them particularly valuable for the study of nonlinear optics at low power levels.

Wang et al. demonstrated microdisk resonators with Q-factors exceeding 10^5 , manufactured through the utilization of dry etching techniques, as evidenced in Fig. 4g [39]. Cheng et al. devised suspended high-Q LN microdisk resonators on SiO_2 substrates through femtosecond laser direct writing, followed by FIB milling, achieving remarkable Q-factors of up to 10^5 [44]. In subsequent research, Cheng et al. further improved the Q-factors of LN microdisk resonators to surpass 10^7 [45]. In more recent developments, Wang et al. employed micro-electro-mechanical systems (MEMS) fabrication techniques to create thin-film LN disk resonators, featuring diameters of $35 \mu\text{m}$ on a silicon platform, and achieved Q-factors of 4.8×10^5 [46]. It's worth noting that presently, Q-factors of resonators based on bulk LN still surpass those of their thin-film counterparts by an order of magnitude. This disparity can be attributed, in part, to the damage introduced during the processing of thin-film LN, primarily arising from ion implantation, as well as surface scattering effects. Yan and colleagues utilized FIB milling technology to fabricate LT microdisk resonators on insulating LT thin films [47]. These microdisk resonators exhibited impressive Q-factors exceeding 10^5 . Furthermore, they managed to achieve a second harmonic output of $2 \mu\text{W}$ under an input power of 500 mW. Notably, the researchers also observed the generation of cascaded third harmonic signals, which holds promise for future integration into lithium tantalate on insulator (LTOI) photonic chips. This work showcases the potential of LTOI microdisk resonators for high-performance nonlinear optical applications.

Zhang and their team successfully fabricated integrated waveguide-coupled microring and racetrack resonators featuring a bending radius of $80 \mu\text{m}$, as visually presented in Fig. 4h [34]. These resonators displayed an exceptional Q-factors of 10^7 and minimal propagation losses of 0.027 dB/cm. Li et al. adopted wet etching to create a micro-racetrack resonator with an intrinsic Q-factors surpassing 9.2×10^6 , as illustrated in Fig. 4i [30]. Importantly, all the

processes involved in this method are CMOS-compatible, making it suitable for integration into existing electronic and photonic systems. Wet etching of thin-film LN allows for the simultaneous processing of multiple chips, substantially enhancing production yield while reducing overall costs. Photonic crystal cavities are renowned for their capacity to simultaneously possess high Q-factors and wavelength-scale mode volumes. Liang and their research group showcased LN photonic crystal nanobeam resonators with optical Q values reaching up to 1.09×10^5 , as depicted in Fig. 4j [40]. This technology opens up avenues for applications demanding high-Q, small-footprint resonators, especially in the context of integrated photonics.

1.5 Electro-optic modulator

EO modulators serve as fundamental components in the realms of optical communication and integrated photonics. These devices are instrumental in the process of modulating high-speed signals, enabling the imposition of information onto the optical carrier wave for transmission within the optical domain. In silicon-based materials, optical modulation relies on the free-carrier plasma dispersion effect, which can lead to challenges such as absorption losses and nonlinear voltage responses [48, 49]. LN has emerged as a material of particular interest due to its remarkable electro-optic performance. LN features a substantial EO coefficient, making it a favored choice for the development of high-performance EO modulators. These LN-based modulators exhibit exceptional voltage-bandwidth characteristics, possess compact form factors, and incur low optical losses. In comparison to silicon-based modulators, they can achieve higher modulation speeds. Consequently, these modulators play an indispensable role in integrated optoelectronics and find widespread applications in optical communication and microwave photonics. Traditionally, LN EO modulators are manufactured using *x*- or *y*-cut LN crystals. These modulators can be broadly categorized into two types based on their operational principles: phase modulators and intensity modulators. Phase modulators function by inducing a phase shift in transmitted light through the alteration of the refractive index via the application of an electric field. They play a fundamental role in photonics and microwave systems. One notable application of LN phase modulators is in the generation of EO frequency combs and frequency shifting [50]. Ren et al. showcased a LN phase modulator characterized by low on-chip optical loss and a low RF half-wave voltage (V_{π}) [51]. The combination of low loss and high RF power-handling capabilities enables the generation of an EO frequency comb with over 40 sidebands using a single modulator. Guarino et al. introduced an EO tunable microring resonator based on LN thin films derived from the smart-cut process, as depicted in Fig. 5a [25]. The EO performance of the LN

microring was assessed by applying a static electric field at the device level, as shown in Fig. 5b. The observed tuning efficiency was approximately 0.105 pm/V. While this value is lower than that of bulk LN devices, it's important to note that the performance of these devices is gradually improving with the advent of high-quality LN single-crystal thin films. This progress holds promise for the development of even more efficient and versatile EO modulators in the future. Mach-Zehnder modulators (MZMs) are the most commonly employed intensity modulators due to their design flexibility and versatility. These MZMs are typically constructed using Mach-Zehnder interferometers integrated with coplanar waveguide electrodes. Wang et al. introduced a monolithic integrated LN EO modulator, as illustrated in Fig. 5c [15]. The modulation region of this device spans a length of 20 cm, featuring a remarkably low half-wave driving voltage of 1.4 V and a half-wave voltage-length product of 2.8 V·cm. These characteristics enable the support of data rates of up to 210 Gbit/s. Additionally, the on-chip optical losses of this platform are less than 0.5 decibels. This LN EO modulator stands out for its CMOS-compatible driving voltages, high integration levels, wide modulation bandwidth, low optical losses, and exceptional signal fidelity. More recently, Li et al. demonstrated an MZM modulator employing diamond-like carbon as a hard mask [27]. This MZM boasted a device length of 1.73 cm and a V_{π} of 1.94 V. EO modulators based on LNOI configurations hold promise as solutions for future direct optoelectronic integration, offering the potential to enhance performance and integration levels.

The combination of two MZMs can be utilized to create an in-phase/quadrature (IQ) modulator. IQ modulators, which encode both amplitude and phase information of light, are essential devices in coherent transmission technology. Xu et al. introduced an IQ modulator based on the LNOI platform, capable of encoding both signal phase and amplitude, as illustrated in Fig. 5d [52]. This device is notable for its low optical losses, low V_{π} , ultra-high EO bandwidth, and a considerably smaller footprint compared to traditional LN devices. It achieved remarkable transmission speeds of up to 320 Gbit/s based on the quadrature amplitude modulation format. Subsequently, the same research team reported the first dual-polarization IQ modulator based on LNOI, as depicted in Fig. 5e [53]. Driven by voltages below 1 V, the device exhibited a record single-carrier net bitrate of 1.96 Tbit/s. Each MZM within the modulator achieved an S21 exceeding 110 GHz at 1 V voltage. The ultra-high bandwidth and exceptionally low power consumption per bit (1.04 fJ/bit) hold significant implications for the development of next-generation EO interfaces.

In addition to MZMs, Michelson interferometer modulators (MIMs) also play a significant role as modulators. Xu et al. demonstrated a MIM based on the heterogeneous silicon/LN platform achieved through BCB bonding,

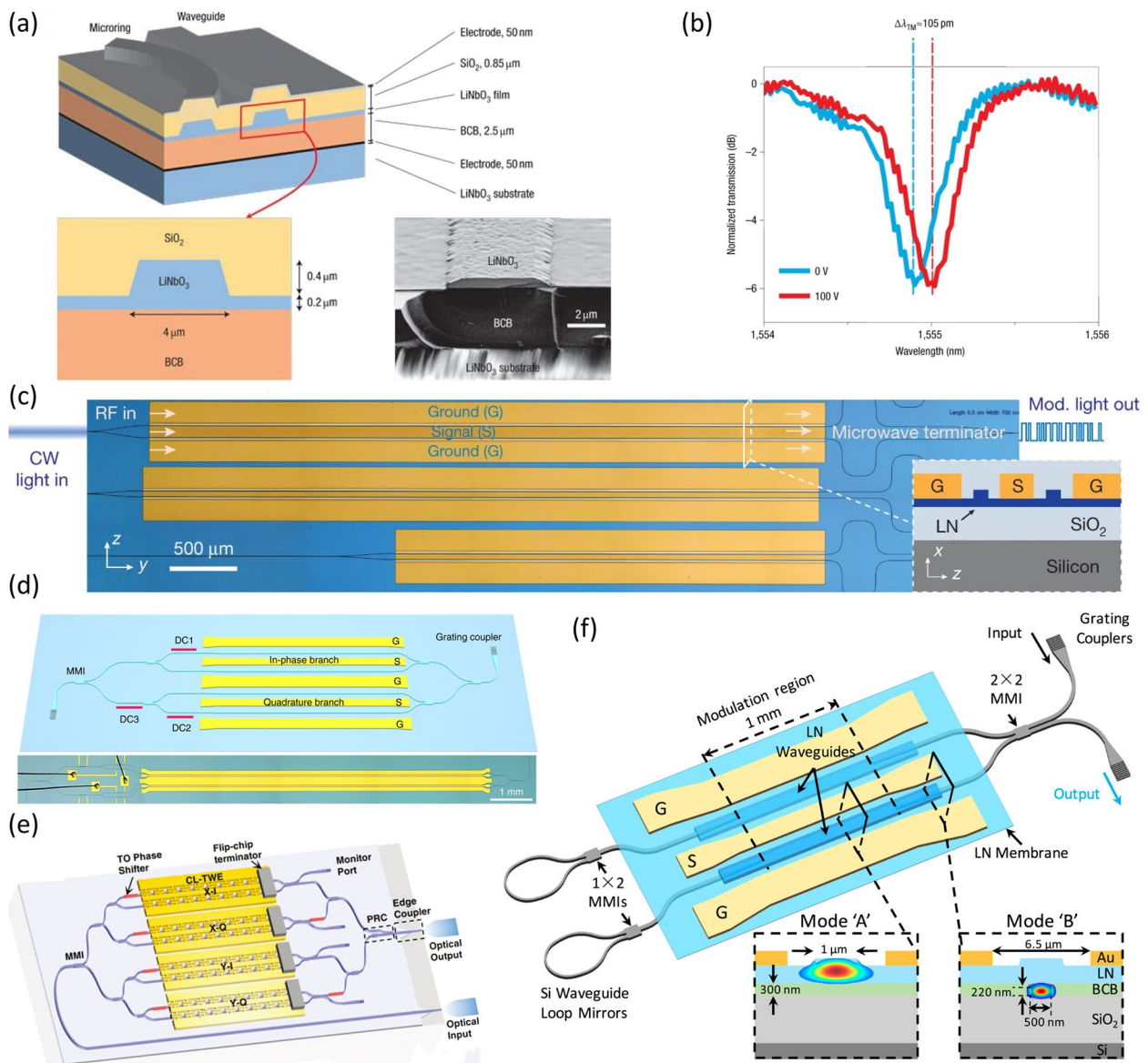


Fig. 5 **a** Cross-section of a LN microring resonator structure. **b** EO shift of the resonance curve. Reprinted by permission from [25] Copyright © 2007, Springer Nature Limited. **c** Microscope image of the fabricated chip consisting of three Mach–Zehnder modulators with various microwave signal line widths and device lengths. Reprinted by permission from [15] Copyright © 2018, Springer Nature Limited.

d IQ modulator on the LNOI platform. Reprinted by permission from [52] Copyright © 2020. **e** Schematic structure of the LN-based IQ modulator. Reprinted by permission from [53] © 2022 Optical Publishing Group. **f** 3D schematic of a heterogeneous silicon/LN MIM. Reprinted by permission from [54] Copyright © 2019

as depicted in Fig. 5f [54]. In comparison to MZMs, this modulator features a reduced half-wave voltage-length product. The modulation region of the device spans 3 mm, and it demonstrates a notably low half-wave voltage-length product of 1.2 V·cm, along with an insertion loss of 3.3 dB. High-speed modulation was successfully demonstrated at data rates of 32 Gbit/s and 40 Gbit/s, featuring impressive extinction ratios of 8 dB and 6.6 dB, respectively. This approach realizes the heterogeneous integration of SOI optical waveguides and LN EO modulators, achieving

exceptional optical modulation characteristics while preserving the advantages of SOI technology. This work represents a significant step forward in the heterogeneous integration of LNOI and SOI technologies. The remarkable progress in dry etching processes has significantly reduced losses in thin-film LN waveguides. Additionally, the rib-loaded waveguide approach has effectively addressed the challenges associated with LN etching processes [6]. Heterogeneous integration with advanced SOI technology is an evident trend in the post-Moore era, facilitating the development of photonic

integrated circuits. Thin-film LN modulators hold a promising future in the domains of microwave photonics and optical communications, offering enhanced performance and versatility.

1.6 Resonators and filters

Wireless communication technology has undergone a significant evolution from 2G to 5G, and as the development of future 6G technologies progresses, there are increased demands on filters, which are core components of the RF frontend in communication devices. Filters play a pivotal role in determining the operating frequency range and bandwidth of these devices. The widespread deployment of 5G and the future advancements in wireless technology place higher demands on filters, requiring characteristics such as high bandwidth, low loss, low temperature drift, and high roll-off coefficients. In the past, two types of acoustic wave-based filters, SAW devices and bulk acoustic wave (BAW) devices, were commonly used in mobile communication devices.

Acoustic resonators are based on the positive/negative piezoelectric effects of piezoelectric materials. Resonance occurs when the frequency of the excitation signal matches the natural frequency, leading to the mutual conversion of electrical and mechanical energy. The mechanical deformation of the material resulting from the positive/negative piezoelectric effects can generate rapidly propagating acoustic waves, including longitudinal waves and transverse waves (shear waves). Among them, shear waves are further classified into vertical shear waves (SV) and horizontal shear waves (SH). On the material surface, the coupling of longitudinal waves and vertical shear waves forms Rayleigh waves, while the coupling of longitudinal waves and horizontal shear waves forms LOVE waves. Both of these acoustic waves belong to surface acoustic waves, constituting the foundation of SAW resonators. Longitudinal waves have a higher velocity compared to these surface waves. Therefore, bulk acoustic wave (BAW) devices based on longitudinal waves are more readily achievable at higher frequencies under the same wavelength.

The structure and piezoelectric materials of piezoelectric resonators determine the acoustical waves or acoustic modes that can be excited within the resonator. Common materials utilized in piezoelectric resonators include AlN, GaN, and LN. In comparison to the former two, LN possesses a higher piezoelectric coupling coefficient, signifying that piezoelectric resonator based on LN can achieve higher k^2 , thereby attaining increased bandwidth. Furthermore, a higher k^2 , in contrast to AlN and GaN devices, also implies higher energy conversion efficiency and lower impedance. LN-based resonators also face certain challenges. For instance, compared to the aforementioned two devices, LN-based devices exhibit

poor temperature stability, slower propagation speed of acoustic waves, and limited power handling capacity due to low thermal conductivity. Additionally, LN is highly anisotropic, making the achievement of optimal performance in LN devices a complex challenge during device design and modeling. Naturally, the presence of more crystal orientations also implies higher degrees of freedom during device design.

Traditional SAW devices consist of two interdigital transducers (IDT) and a piezoelectric film. Generally, these devices are not suitable for frequencies above 2.5G and exhibit performance degradation with increasing temperature. Consequently, temperature-compensated SAW (TC-SAW) has been developed, incorporating a thin layer of SiO₂ to achieve temperature compensation [55]. Furthermore, the performance of traditional SAW is constrained by the relatively low surface acoustic velocity of LN. In contrast, the incredible high-performance SAW (I.H.P.SAW) achieves higher frequencies by introducing a high-velocity layer and a functional layer beneath the piezoelectric layer [56, 57]. This enhancement successfully extends the operating frequency of SAW devices to around 3.5 GHz, making it comparable to conventional BAW devices.

BAW devices are structured as a sandwich of upper and lower electrodes with a piezoelectric material in between, primarily categorized into solidly mounted type resonator (SMR-BAW) and thin film bulk acoustic resonator (FBAR). The key distinction lies in the reflective boundary: the former utilizes a Bragg reflector layer, while the latter uses the solid-air interface as the reflective boundary. Compared to SMR-BAW, FBAR exhibits higher working frequencies, superior temperature characteristics, lower insertion loss, higher power handling capacity, and cost advantages. Currently, FBARs based on AlN or AlScN have been successfully commercialized.

The lateral field excited bulk acoustic wave resonators (XBAR), tailored to meet the stringent demands of the 5G market, has emerged as an alternative solution. LN is an exceptional ferroelectric material with a high piezoelectric coefficient, offering significant advantages in creating resonators with high coupling coefficients and high-bandwidth filters. This makes XBARs based on LN a promising option for meeting the demands of high-frequency communication applications. LN has a long history of use in SAW devices, dating back to the last century. However, the progress in developing LN devices was hampered by challenges related to the quality of deposited LN thin films and the lack of effective transfer technologies. The introduction of Smart-cut technology has revolutionized the field by enabling the bonding of high-quality single-crystal LN/LT thin films to other substrates. This breakthrough has led to a significant

surge in research on acoustic resonators based on single-crystal LN/LT thin films [29, 58–61].

LN crystals exhibit pronounced anisotropy, with distinct atomic arrangements on different crystal planes. This results in significant variations in the properties of LN on different crystal facets, such as the piezoelectric coefficient (e), dielectric constant (ϵ), and others. These factors impact performance metrics like acoustic velocity and electromechanical coupling coefficients. The acoustic properties, such as phase velocity and k^2 , can vary significantly for a specific mode depending on the orientation and cut of the LN material. For instance, the commonly chosen orientation for Thin Film Bulk Acoustic Resonators (FBAR) is y -36. Thickness shear waves primarily utilize e_{15} , which is more pronounced in the z and y -128 orientations. Horizontal shear waves primarily utilize e_{16} , and orientations such as y -36, x , and y are more suitable. However, practical device design not only considers the piezoelectric coefficients on different crystal orientations but also accounts for the influence of factors like acoustic velocity. Among the various cut angles and acoustic modes in LN, the anti-symmetric Lamb wave mode based on z -cut LN resonators stands out due to its high resonance frequency and k^2 . This mode is particularly valuable for enhancing filter performance by increasing the center frequency, relative bandwidth, and reducing insertion loss. Notably, XBARs offer distinct advantages in the current 5G RF domain, including high resonance frequencies ranging from 3 to 80 GHz, high bandwidth, and a high Q-factor, which translates to low insertion losses (less than 2 dB). This makes XBARs a highly promising technology for addressing the demanding requirements of modern 5G wireless communication. Yan et al. employed the Smart-cut process to transfer a y -cut LT single crystal thin film with a thickness of 510 nm onto a Si substrate, culminating in the fabrication of a single-port SAW device operating at a fundamental frequency of 350 MHz [62]. Wu et al. harnessed the smart-cut process to create a 4-inch LT/SiO₂/sapphire substrate structure [63]. The propagation loss within the LTOI platform was measured at 2.95 dB/mm. On the foundation of the LTOI structure, a shear horizontal SAW resonator was developed, demonstrating a resonant frequency of 1.76 GHz and an impressive maximum Q-factors of 4421. It is noteworthy that LTOI stands as a promising high-performance filter platform in the context of 5G communication era. This versatile material system has the potential to serve as an exceptional candidate for advanced filtering applications. Furthermore, Assila et al. undertook the production of high-frequency resonators, utilizing the first-order antisymmetric Lamb wave mode (A1) [64]. These resonators attained an exceptional resonant frequency of 5 GHz, positioning them as noteworthy components in the high-frequency spectrum.

In 2008, Kadota et al. first fabricated a Lamb wave resonator using LN thin film, with a resonant frequency of 4.5 GHz [65]. However, due to the poor quality of LN thin films prepared by chemical vapor deposition, the device exhibited suboptimal performance. Subsequently, Yang et al. demonstrated C-band (4–8 GHz) LN ladder filters based on the A1 mode [66]. These resonators and filters were fabricated on a 500 nm thick z -cut LN thin film. The filter comprised resonators based on the first-order asymmetric Lamb wave mode in thin-film LN. These resonators exhibited a coupling coefficient of 28% and a quality factor of 420. The fabricated filters demonstrated large fractional bandwidths (> 8.5%), low insertion loss (IL < 2.7 dB), flat in-band group delays, and spurious-free responses. Plessky et al. proposed an XBAR fabricated using MEMS and photolithography processes, as illustrated in Fig. 6a [67]. They observed the 3rd, 5th, 7th, and 9th harmonics, reaching frequencies of up to 38 GHz, which holds promise for high-frequency filter design. Turner et al. designed and manufactured an XBAR filter with a frequency of 4.7 GHz and a bandwidth of 600 MHz, as shown in Fig. 6b and c [59]. Furthermore, Assila et al. used a 400 nm thick 42° y -cut LT thin film to fabricate an A1 mode XBAR with a resonant frequency of 5 GHz, a relative bandwidth of 7.3%, and an impedance ratio of 72 dB. This work demonstrated that LT can also be utilized for high-frequency devices in the A1 Lamb wave mode. XBAR filters based on LN/LT thin films offer high-frequency and high coupling coefficients that cannot be achieved by SAW and BAW, making them promising candidates for high-performance resonators/filters in the 5G and 6G frequency bands.

1.7 Quantum devices

Quantum technology has experienced rapid development in recent years, with widespread applications in quantum communication, quantum computing, quantum precision measurement, and more. Much of the progress in quantum technology is underpinned by the advancements in traditional classical techniques and materials. Two such materials, LN/LT, which are commonly used in classical optics, have also shown considerable potential in the field of quantum optics. In particular, LN plays a crucial role in efficiently generating quantum optical signals through second-order nonlinear processes such as sum frequency generation (SFG), difference frequency generation (DFG), and spontaneous parametric down-conversion (SPDC). These processes have enabled applications like single-photon frequency conversion. The optimization of LN waveguides and the development of phase-matching techniques have significantly improved the efficiency of nonlinear conversion processes, providing a strong foundation for the quantum applications of LN.

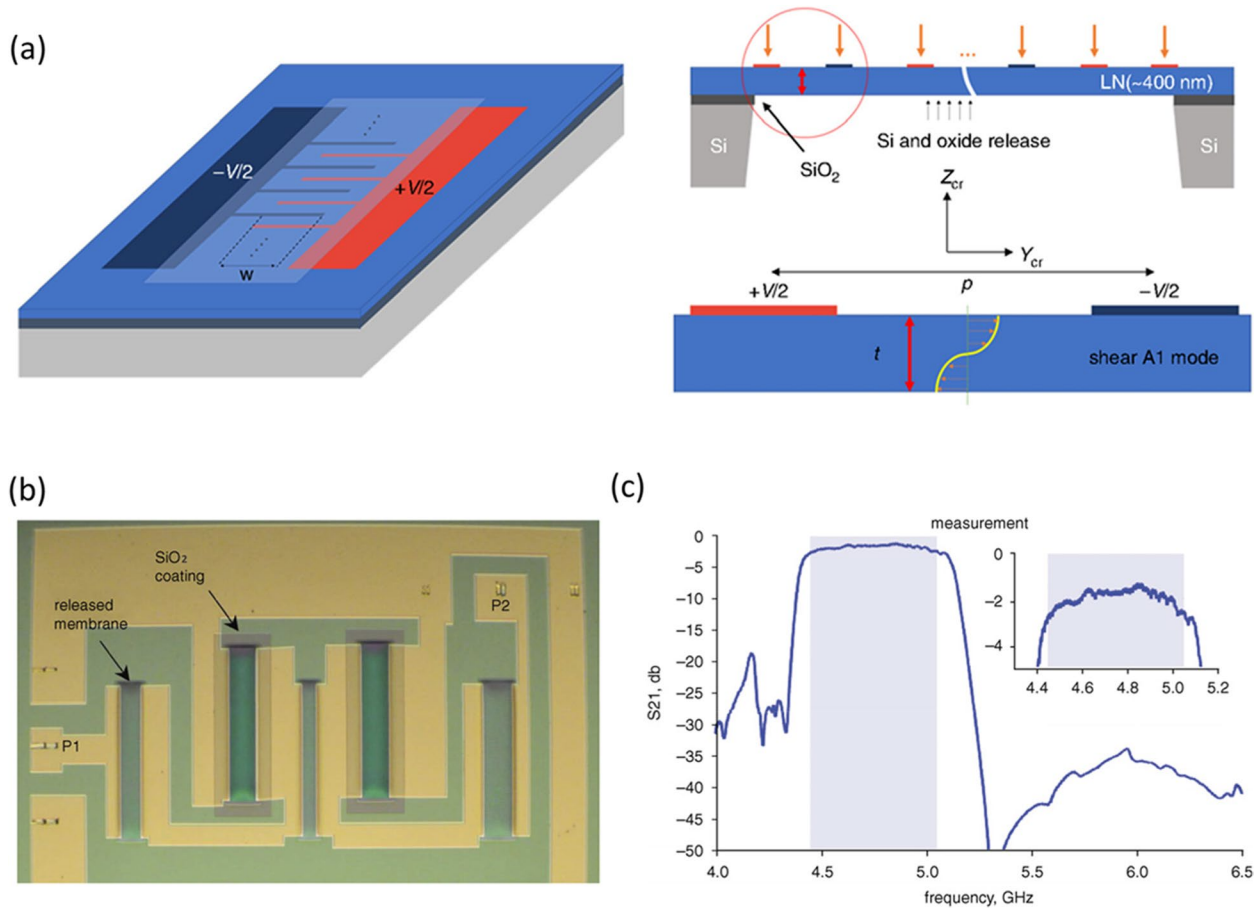


Fig. 6 **a** Schematic of the device structure. Reprinted by permission from [67] © 2020 The Institution of Engineering and Technology. **b** Microscope image of a prototype 5-resonator XBAR ladder filter. **c**

Filter performance measurement curve. Reprinted by permission from [59] © 2020 The Institution of Engineering and Technology

Quantum light sources are critical components for various applications in the quantum field, typically encompassing single-photon sources and entangled photon sources. The utilization of the SPDC process within LN presents a promising approach for generating quantum light sources [12]. Zhu et al. achieved on-chip generation and manipulation of entangled photons using a LN photonics chip, as illustrated in Fig. 7a [68]. This chip integrates functionalities like entangled photon sources, photon interferometers, and EO modulators on the same substrate, enabling efficient generation and rapid switching of two-path entangled photon states. The photon flux reaches approximately 1.4×10^7 pairs $\text{nm}^{-1}\text{mW}^{-1}$. Subsequently, the same team extended their work to titanium-diffused LN waveguides, successfully generating non-degenerate polarization-entangled photon pairs for optical fiber communication, with an interference visibility exceeding 90%.

In recent years, research on quantum light source devices based on LN thin films has gained significant attention. Ma et al. demonstrated high-rate and high-quality photon-pair and heralded single-photon generation using a

z-cut periodically-poled LN microring resonator [73]. The device achieved photon-pair generation at high rates using low pump power. Cheng et al. proposed a chip-scale hybrid waveguide structure, combining Si_3N_4 and thin film periodically-poled LN, allowing for the generation of highly pure photons and wafer-scale integration, as shown in Fig. 7b [69]. This hybrid waveguide chip can produce high-purity type-II SPDC photon sources for quantum communication, quantum key distribution, and large-scale quantum information processing. In the realm of quantum information, high-performance single-photon detectors hold great importance for achieving long-distance quantum key distribution. Tang et al. have demonstrated efficient waveguide-integrated superconducting nanowire single-photon detectors on thin-film LN, as depicted in Fig. 7c [70]. These devices were fabricated using commercially available z-cut LN single-crystal thin films produced by NanoLN company. They exhibited an on-chip detection efficiency of 46%, a dark count rate of 13 Hz, a timing jitter of 32 ps, and a noise equivalent power of 1.42×10^{-18} W/ $\sqrt{\text{Hz}}$. This achievement offers a new approach to generating,

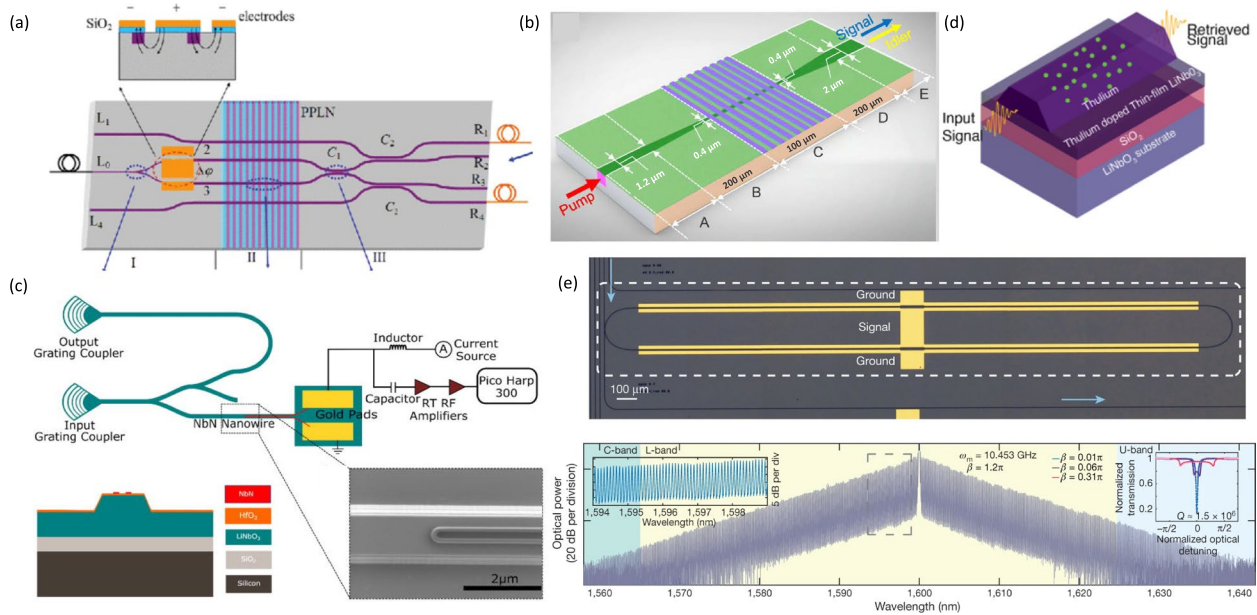


Fig. 7 **a** Schematic diagram of a LN photonic chip. Reprinted by permission from [68] © 2014 American Physical Society. **b** Illustration of chip-scale hybrid Si-rich silicon nitride and thin film PPLN waveguide structure. Reprinted by permission from [69] © 2019 Optical Society of America. **c** LN-based single-photon detector. Reprinted by permission from [70] © 2023 Copyright, AIP Publish-

ing. **d** Schematic of the device structure composed of a thin-film LN waveguide doped with thulium rare-earth ions. Reprinted by permission from [71] Copyright © 2023, American Chemical Society. **e** EO comb. Reprinted by permission from [72] Copyright © 2019, Springer Nature Limited

manipulating, and measuring quantum light on compact integrated platforms. In the context of remote quantum communication and networking, there is a growing need for storing quantum states. Quantum memory serves as a crucial component of optical quantum computers and quantum networks. Waveguides based on LN have shown substantial advantages in quantum storage applications. Recently, Dutta et al. demonstrated a compact chip-integrated atomic frequency comb memory in rare-earth-doped thin-film LN, as illustrated in Fig. 7d [71]. This optical memory exhibited a broad storage bandwidth exceeding 100 MHz and an optical storage time of up to 250 ns. Such a quantum memory can serve as a fundamental component of high-bandwidth quantum information processors on a chip. Kerr frequency combs are generated in microresonators using nonlinear optical effects to produce a series of equidistant frequency components, resulting in a comb-like spectrum. Kerr microresonator frequency combs are characterized by their discrete, equidistant frequencies and high repetition rates. They find extensive applications and prospects in various fields such as laser technology, metrology, spectroscopy, quantum entanglement sources, and more. The integration of Kerr frequency combs on-chip, where the resonator and pump light source are combined on the same chip, reduces the size, power consumption, and enhances reliability and repeatability. LN is used to prepare Kerr frequency combs due to its significant third-order nonlinear optical effects.

Wang et al. demonstrated Kerr frequency combs based on LN and have performed spectral and temporal manipulation of the comb signals. This approach offers compact solutions for various applications. Moreover, the high EO effect of LN enables the creation of EO frequency combs, allowing for rapid tunability of the repetition frequency. As shown in Fig. 7e, Zhang et al. achieved monolithic integration of an EO comb generator on a LN thin-film photonics platform [72]. Compared to bulk EO combs and EO combs based on indium phosphide and silicon platforms, the performance is significantly superior. The remarkable reconfigurability of Kerr combs is a powerful addition, offering more possibilities for broadening the optical applications of frequency combs.

2 Conclusion and perspectives

This review offers an overview of the latest advancements in LN/LT single-crystal thin films, encompassing material properties, processing techniques, and the diverse array of functional devices they enable. With the evolution of large-size wafers and the production of high-quality single-crystal thin films, LN/LT have exhibited remarkable advantages across a broad spectrum of application scenarios. These materials, holding a pivotal position in the optical era, empower the realization of various optical functionalities

and structures. They also facilitate hybrid integration with other platforms and quantum applications, playing an indispensable role in chip applications for the post-Moore era.

In the post-Moore era, the advancement of chip performance is no longer reliant solely on the reduction of device size. It necessitates the exploration of various technological approaches, which encompass novel materials, innovative device types, and new architectural paradigms. Over recent decades, the introduction of LN/LT, along with their single-crystal thin films, has exerted a profound influence on the progression of photonics. Leveraging their versatility, capacity for strong light confinement, and design flexibility, particularly in the case of LN single-crystal thin films, they function as a universal platform for integrated optics. The ongoing emergence of novel and prospective applications continues to kindle research enthusiasm in the realm of LN/LT single-crystal thin films or LNOI/LTOI devices. These materials enable the development of high-speed, low-power, and highly integrated EO modulators, serving the requisites of future data transmission and processing, particularly in domains such as optical communication, data centers, and artificial intelligence. At present, 800 Gbit/s LN EO modulators have made their entry into the market. Furthermore, they are instrumental in facilitating efficient, broadband, and multifunctional nonlinear optical devices, catering to the demands of quantum operations and frequency conversion in fields like quantum computing, quantum communication, and optical frequency combs. In addition, high-sensitivity, high-speed, and multi-mode acousto-optic modulators based on these materials can fulfill the necessities of photonics in the realms of microwave applications, radar signal processing, wireless communication, and other domains. These applications underscore the substantial potential and value of LN/LT single-crystal thin films in post-Moore era chips. Nevertheless, there still exist technical challenges and impediments that need to be addressed. These include refining the fabrication processes of LN/LT single-crystal thin films, perfecting hybrid integration techniques, and advancing device design methodologies.

The realization of integrated optics using LNOI and LTOI necessitates the preparation of these materials as single-crystal thin films, which are subsequently transferred onto other substrates. Presently, the commonly employed methods for fabrication entail processes like thinning, polishing, and bonding to attain the desired thickness and quality of single-crystal thin films. However, there exist several challenges that need to be addressed. Commercially produced LNOI/LTOI wafers are predominantly available in sizes below 6 inches, and they encounter issues such as high production costs, low yields, and quality variability. The limited wafer sizes and high costs render LNOI and LTOI less competitive when compared to more established materials like Si_xN_y and SOI. Therefore, the imperative

task is to establish an efficient, low-loss, low-defect, low-stress, and cost-effective fabrication process while maintaining the performance of single-crystal thin films. This imperative necessitates the continuous refinement of existing processing equipment, including thinning machines, polishing machines, and bonding machines, with the aim of reducing production costs and complexity, ensuring wafer flatness and uniformity, and scaling up production capacity. Microfabrication of LNOI/LTOI single-crystal thin films is also a critical technological aspect, as it profoundly influences the morphology, dimensions, and precision of the devices. Various microfabrication methods are currently in use, each characterized by distinct attributes. Dry etching, for example, is known for its high precision but is associated with high costs and slow processing speeds. It yields smooth sidewalls and is particularly suitable for applications where high etching precision is imperative. However, it can be hindered by its processing speed, especially when producing ridge structures with a minimum feature size of a few hundred nanometers, which often necessitates the use of EBL for patterning photoresist, limiting production speed. Developing wafer-level lithography techniques could offer a potential solution. Wet etching, on the other hand, is characterized by lower costs and faster processing speeds but typically results in lower etching precision and rough sidewalls. The choice of appropriate microfabrication methods, the optimization of etching parameters, the improvement of etching uniformity and selectivity, and the reduction of etching losses and defects are areas that demand ongoing exploration and enhancement.

The design and processing of LNOI and LTOI can be compatible and seamlessly integrated with other materials and platforms to enable the creation of more intricate and diverse functionalities. The progress and innovations in mixed integration techniques for LNOI and LTOI can facilitate efficient compatibility and interoperability with platforms such as Si-based, Si_xN_y , and indium phosphide. This compatibility paves the way for the construction of multifunctional, multi-wavelength, and multi-mode photonic chips. The primary challenge in achieving this lies in ensuring high efficiency and low losses at the interfaces and couplings while addressing potential material incompatibilities. A noteworthy recent development in this context was demonstrated by IBM and the Swiss Federal Institute of Technology Lausanne, where they introduced a heterogeneous wafer-scale platform, $\text{Si}_3\text{N}_4/\text{LN}$. This platform integrates ultra-low-loss Si_3N_4 waveguides with thin-film LN, enabling the realization of hybrid self-injection-locked lasers [74]. With ongoing refinement of photonic circuit design and process enhancements, such heterogeneous platforms are anticipated to find broader and more diverse applications in the future. Materials like LN and LT encompass a multitude of EO properties, leading to

a wide range of optical applications that meet practical requirements. Their significance in the realm of photonics is comparable to that of silicon in the field of electronics. LN and LT have already emerged as foundational materials in the development of integrated photonics for the future.

Authors' contributions Yixin Zhu: Writing-original draft. Qing Wan: Writing-review & editing.

Funding This study was supported by Key R&D Program of Zhejiang (Grant Nos. 2024SSYS0043, the National Natural Science Foundation of China (Grant Nos. 61921005, 62074075) and Zhejiang Province introduces and cultivates leading innovation and entrepreneurship teams (Grant Nos. 2023TD1035).

Availability of data and materials Data sharing not applicable to this article as no datasets were generated or analysed during the current study.

Declarations

Competing interests Author Qing Wan is an editorial board member.

Open Access This article is licensed under a Creative Commons Attribution 4.0 International License, which permits use, sharing, adaptation, distribution and reproduction in any medium or format, as long as you give appropriate credit to the original author(s) and the source, provide a link to the Creative Commons licence, and indicate if changes were made. The images or other third party material in this article are included in the article's Creative Commons licence, unless indicated otherwise in a credit line to the material. If material is not included in the article's Creative Commons licence and your intended use is not permitted by statutory regulation or exceeds the permitted use, you will need to obtain permission directly from the copyright holder. To view a copy of this licence, visit <http://creativecommons.org/licenses/by/4.0/>.

References

- Boes A, Corcoran B, Chang L et al (2018) Status and potential of lithium niobate on insulator (Inoi) for photonic integrated circuits. *Laser & Photonics Reviews* 12(4):1700256. <https://doi.org/10.1002/lpor.201700256>
- Yuan S, Hu C, Pan A et al (2021) Photonic devices based on thin-film lithium niobate on insulator. *J Semicond* 42(4):041304. <https://doi.org/10.1088/1674-4926/42/4/041304>
- Zhu D, Shao L, Yu M et al (2021) Integrated photonics on thin-film lithium niobate. *Adv Opt Photon* 13(2):242–352. <https://doi.org/10.1364/AOP.411024>
- Guanyu C, Nanxi L, Da Jun N et al (2022) Advances in lithium niobate photonics: Development status and perspectives. *Advanced Photonics* 4(3):034003. <https://doi.org/10.1117/1.AP.4.3.034003>
- Qi Y, Li Y (2020) Integrated lithium niobate photonics. *Nanophotonics* 9(6):1287–1320. <https://doi.org/10.1515/nanoph-2020-0013>
- Jia Y, Wang L, Chen F (2021) Ion-cut lithium niobate on insulator technology: Recent advances and perspectives. *Appl Phys Rev* 8(1):011307. <https://doi.org/10.1063/5.0037771>
- Wan Q, Wang L, Liu W et al (2001) Investigation of h^+ and b^+/h^+ implantation in LiTaO_3 single-crystals. *Nuclear Instruments and Methods in Physics Research Section B: Beam Interactions with Materials and Atoms*. 184(4):531–535. [https://doi.org/10.1016/S0168-583X\(01\)00827-8](https://doi.org/10.1016/S0168-583X(01)00827-8)
- Aspar B, Moriceau H, Jalaguier E et al (2001) The generic nature of the smart-cut® process for thin film transfer. *J Electron Mater* 30(7):834–840. <https://doi.org/10.1007/s11664-001-0067-2>
- Wang C, Li Z, Kim M-H et al (2017) Metasurface-assisted phase-matching-free second harmonic generation in lithium niobate waveguides. *Nat Commun* 8(1):2098. <https://doi.org/10.1038/s41467-017-02189-6>
- Niu Y, Lin C, Liu X et al (2020) Optimizing the efficiency of a periodically poled Inoi waveguide using in situ monitoring of the ferroelectric domains. *Appl Phys Lett* 116(10):101104. <https://doi.org/10.1063/1.5142750>
- Xue G-T, Niu Y-F, Liu X et al (2021) Ultrabright multiplexed energy-time-entangled photon generation from lithium niobate on insulator chip. *Phys Rev Appl* 15(6):064059. <https://doi.org/10.1103/PhysRevApplied.15.064059>
- Zhao J, Ma C, Rüsing M et al (2020) High quality entangled photon pair generation in periodically poled thin-film lithium niobate waveguides. *Phys Rev Lett* 124(16):163603. <https://doi.org/10.1103/PhysRevLett.124.163603>
- Wang C, Zhang M, Yu M et al (2019) Monolithic lithium niobate photonic circuits for kerr frequency comb generation and modulation. *Nat Commun* 10(1):978. <https://doi.org/10.1038/s41467-019-08969-6>
- Desiatov B, Shams-Ansari A, Zhang M et al (2019) Ultra-low-loss integrated visible photonics using thin-film lithium niobate. *Optica* 6(3):380–384. <https://doi.org/10.1364/OPTICA.6.000380>
- Wang C, Zhang M, Chen X et al (2018) Integrated lithium niobate electro-optic modulators operating at cmos-compatible voltages. *Nature* 562(7725):101–104. <https://doi.org/10.1038/s41586-018-0551-y>
- Wang T-J, Chu C-H, Lin C-Y (2007) Electro-optically tunable microring resonators on lithium niobate. *Opt Lett* 32(19):2777–2779. <https://doi.org/10.1364/OL.32.002777>
- Sakashita Y, Segawa H (1995) Preparation and characterization of LiNbO_3 thin films produced by chemical-vapor deposition. *J Appl Phys* 77(11):5995–5999. <https://doi.org/10.1063/1.359183>
- Lansiaux X, Dogheche E, Remiens D et al (2001) LiNbO_3 thick films grown on sapphire by using a multistep sputtering process. *J Appl Phys* 90(10):5274–5277. <https://doi.org/10.1063/1.1378332>
- Nakata Y, Gunji S, Okada T et al (2004) Fabrication of LiNbO_3 thin films by pulsed laser deposition and investigation of nonlinear properties. *Appl Phys A* 79(4):1279–1282. <https://doi.org/10.1007/s00339-004-2748-1>
- Yoon JG, Kim K (1996) Growth of highly textured LiNbO_3 thin film on si with mgo buffer layer through the sol-gel process. *Appl Phys Lett* 68(18):2523–2525. <https://doi.org/10.1063/1.115842>
- Gitmans F, Sitar Z, Günter P (1995) Growth of tantalum oxide and lithium tantalate thin films by molecular beam epitaxy. *Vacuum*. 46(8):939–942. [https://doi.org/10.1016/0042-207X\(95\)00077-1](https://doi.org/10.1016/0042-207X(95)00077-1)
- Levy M, Osgood RM Jr, Liu R et al (1998) Fabrication of single-crystal lithium niobate films by crystal ion slicing. *Appl Phys Lett* 73(16):2293–2295. <https://doi.org/10.1063/1.121801>
- Hui, H., Li, G., Raimund, R., et al. Towards nonlinear photonic wires in lithium niobate. *ProcSPIE*. 7604(76040R) (2010). <https://doi.org/10.1117/12.842674>
- Poberaj G, Hu H, Sohler W et al (2012) Lithium niobate on insulator (Inoi) for micro-photonic devices. *Laser & Photonics Reviews*. 6(4):488–503. <https://doi.org/10.1002/lpor.201100035>

25. Guarino A, Poberaj G, Rezzonico D et al (2007) Electro–optically tunable microring resonators in lithium niobate. *Nat Photonics* 1(7):407–410. <https://doi.org/10.1038/nphoton.2007.93>
26. Chen G, Cheung EJH, Cao Y et al (2021) Analysis of perovskite oxide etching using argon inductively coupled plasmas for photonics applications. *Nanoscale Res Lett* 16(1):32. <https://doi.org/10.1186/s11671-021-03494-2>
27. Li Z, Wang RN, Lihachev G et al (2023) High density lithium niobate photonic integrated circuits. *Nat Commun* 14(1):4856. <https://doi.org/10.1038/s41467-023-40502-8>
28. Gong S, Piazza G (2013) Design and analysis of lithium–niobate-based high electromechanical coupling rf-mems resonators for wideband filtering. *IEEE Trans Microw Theory Tech* 61(1):403–414. <https://doi.org/10.1109/TMTT.2012.2228671>
29. Gong S, Piazza G (2013) Figure-of-merit enhancement for laterally vibrating lithium niobate mems resonators. *IEEE Trans Electron Devices* 60(11):3888–3894. <https://doi.org/10.1109/TEDE.2013.2281734>
30. Zhuang R, He J, Qi Y et al (2023) High-Q thin-film lithium niobate microrings fabricated with wet etching. *Advanced Materials* 35(3):2208113. <https://doi.org/10.1002/adma.202208113>
31. Dawar AL, Al-Shukri SM, De La Rue RM et al (1986) Fabrication and characterization of titanium-indiffused proton-exchanged optical waveguides in γ -LiNbO₃. *Appl Opt* 25(9):1495–1498. <https://doi.org/10.1364/AO.25.001495>
32. Krasnokutska I, Tambasco J-LJ, Li X et al (2018) Ultra-low loss photonic circuits in lithium niobate on insulator. *Opt Express* 26(2):897–904. <https://doi.org/10.1364/OE.26.000897>
33. Wolf R, Breunig I, Zappe H et al (2018) Scattering-loss reduction of ridge waveguides by sidewall polishing. *Opt Express* 26(16):19815–19820. <https://doi.org/10.1364/OE.26.019815>
34. Zhang M, Wang C, Cheng R et al (2017) Monolithic ultra-high-Q lithium niobate microring resonator. *Optica* 4(12):1536–1537. <https://doi.org/10.1364/OPTICA.4.001536>
35. Wu R, Wang M, Xu J et al. Long low-loss-litium niobate on insulator waveguides with sub-nanometer surface roughness. *Nanomaterials* 8(11), (2018). <https://doi.org/10.3390/nano8110910>
36. Lu Y, Johnston B, Dekker P et al. Channel waveguides in lithium niobate and lithium tantalate. *Molecules* 25(17), (2020). <https://doi.org/10.3390/molecules25173925>
37. Nishi H, Tsuchizawa T, Segawa T et al. Low-loss lithium tantalate on insulator waveguide towards on-chip nonlinear photonics. 2022 27th OptoElectronics and Communications Conference (OECC) and 2022 International Conference on Photonics in Switching and Computing (PSC). 1–3 (2022). <https://doi.org/10.23919/OECC/PSC53152.2022.9850122>
38. Jin T, Zhou J, Lin PT (2019) Mid-infrared electro-optical modulation using monolithically integrated titanium dioxide on lithium niobate optical waveguides. *Sci Rep* 9(1):15130. <https://doi.org/10.1038/s41598-019-51563-5>
39. Wang C, Burek MJ, Lin Z et al (2014) Integrated high quality factor lithium niobate microdisk resonators. *Opt Express* 22(25):30924–30933. <https://doi.org/10.1364/OE.22.030924>
40. Liang H, Luo R, He Y et al (2017) High-quality lithium niobate photonic crystal nanocavities. *Optica* 4(10):1251–1258. <https://doi.org/10.1364/OPTICA.4.001251>
41. Wang Y, Chen Z, Cai L et al (2017) Amorphous silicon-lithium niobate thin film strip-loaded waveguides. *Opt Mater Express* 7(11):4018–4028. <https://doi.org/10.1364/OME.7.004018>
42. Ahmed ANR, Shi S, Zablocki M et al (2019) Tunable hybrid silicon nitride and thin-film lithium niobate electro-optic micro-resonator. *Opt Lett* 44(3):618–621. <https://doi.org/10.1364/OL.44.000618>
43. Jiang X-F, Zou C-L, Wang L et al (2016) Whispering-gallery microcavities with unidirectional laser emission. *Laser & Photonics Reviews*. 10(1):40–61. <https://doi.org/10.1002/lpor.201500163>
44. Lin J, Xu Y, Fang Z et al (2015) Fabrication of high-Q lithium niobate microresonators using femtosecond laser micromachining. *Sci Rep* 5(1):8072. <https://doi.org/10.1038/srep08072>
45. Wu R, Zhang J, Yao N et al (2018) Lithium niobate micro-disk resonators of quality factors above 107. *Opt Lett* 43(17):4116–4119. <https://doi.org/10.1364/OL.43.004116>
46. Wang, R., Bhave, S. A. Lithium niobate optomechanical disk resonators. 2020 Joint Conference of the IEEE International Frequency Control Symposium and International Symposium on Applications of Ferroelectrics (IFCS-ISAF). 1–4 (2020). <https://doi.org/10.1109/IFCS-ISAF41089.2020.9264025>
47. Yan X, Liu Y, Ge L et al (2020) High optical damage threshold on-chip lithium tantalate microdisk resonator. *Opt Lett* 45(15):4100–4103. <https://doi.org/10.1364/OL.394171>
48. Xu Q, Schmidt B, Pradhan S et al (2005) Micrometre-scale silicon electro-optic modulator. *Nature* 435(7040):325–327. <https://doi.org/10.1038/nature03569>
49. Sinatkas G, Christopoulos T, Tsilipakos O et al (2021) Electro-optic modulation in integrated photonics. *J Appl Phys* 130(1):010901. <https://doi.org/10.1063/5.0048712>
50. Wright LJ, Karpiński M, Söller C et al (2017) Spectral shearing of quantum light pulses by electro-optic phase modulation. *Phys Rev Lett* 118(2):023601. <https://doi.org/10.1103/PhysRevLett.118.023601>
51. Ren T, Zhang M, Wang C et al (2019) An integrated low-voltage broadband lithium niobate phase modulator. *IEEE Photonics Technol Lett* 31(11):889–892. <https://doi.org/10.1109/LPT.2019.2911876>
52. Xu M, He M, Zhang H et al (2020) High-performance coherent optical modulators based on thin-film lithium niobate platform. *Nat Commun* 11(1):3911. <https://doi.org/10.1038/s41467-020-17806-0>
53. Xu M, Zhu Y, Pittalà F et al (2022) Dual-polarization thin-film lithium niobate in-phase quadrature modulators for terabit-per-second transmission. *Optica* 9(1):61–62. <https://doi.org/10.1364/OPTICA.449691>
54. Xu M, Chen W, He M et al (2019) Michelson interferometer modulator based on hybrid silicon and lithium niobate platform. *APL Photonics* 4(10):100802. <https://doi.org/10.1063/1.5115136>
55. Liu Y, Liu J, Wang Y et al (2019) A novel structure to suppress transverse modes in radio frequency tc-saw resonators and filters. *IEEE Microwave Wirel Compon Lett* 29(4):249–251. <https://doi.org/10.1109/LMWC.2019.2898730>
56. Kimura T, Omura M, Kishimoto Y et al. A high velocity and wide-band saw on a thin LiNbO₃ plate bonded on a si substrate in the shf range. 2019 IEEE International Ultrasonics Symposium (IUS). 1239–1248 (2019). <https://doi.org/10.1109/ULTSYM.2019.8926065>
57. Takai T, Iwamoto H, Takamine Y et al. I.H.P. Saw technology and its application to microacoustic components (invited). 2017 IEEE International Ultrasonics Symposium (IUS). 1–8 (2017). <https://doi.org/10.1109/ULTSYM.2017.8091876>
58. Song YH, Gong S (2015) Elimination of spurious modes in sh0 lithium niobate laterally vibrating resonators. *IEEE Electron Device Lett* 36(11):1198–1201. <https://doi.org/10.1109/LED.2015.2478378>
59. Turner PJ, Garcia B, Yantchev V et al (2019) 5 GHz band n79 wideband microacoustic filter using thin lithium niobate membrane. *Electronics Letters*. 55(17):942–944. <https://doi.org/10.1049/el.2019.1658>
60. Kimura T, Omura M, Kishimoto Y et al (2019) Comparative study of acoustic wave devices using thin piezoelectric plates in the 3–5-GHz range. *IEEE Trans Microw Theory Tech* 67(3):915–921. <https://doi.org/10.1109/TMTT.2018.2890661>

61. Yang Y, Lu R, Gong S (2020) High Q antisymmetric mode lithium niobate mems resonators with spurious mitigation. *J Microelectromech Syst* 29(2):135–143. <https://doi.org/10.1109/JMEMS.2020.2967784>
62. Yan Y, Huang K, Zhou H et al (2019) Wafer-scale fabrication of 42° rotated y-cut LiTaO₃-on-insulator (ltoi) substrate for a saw resonator. *ACS Appl Electron Mater* 1(8):1660–1666. <https://doi.org/10.1021/acsaelm.9b00351>
63. Wu J, Zhang S, Chen Y et al (2022) Advanced surface acoustic wave resonators on LiTaO₃/SiO₂/sapphire substrate. *IEEE Electron Device Lett* 43(10):1748–1751. <https://doi.org/10.1109/LED.2022.3200418>
64. Assila N, Kadota M, Tanaka S (2019) High-frequency resonator using a1 lamb wave mode in LiTaO₃ plate. *IEEE Trans Ultrason Ferroelectr Freq Control* 66(9):1529–1535. <https://doi.org/10.1109/TUFFC.2019.2923579>
65. Kadota M, Ogami T, Yamamoto K et al (2009) High-frequency lamb wave device composed of LiNbO₃ thin film. *Japanese Journal of Applied Physics* 48(7S):07GG08. <https://doi.org/10.1143/JJAP.48.07GG08>
66. Yang Y, Lu R, Gao L et al (2019) 4.5 GHz lithium niobate mems filters with 10% fractional bandwidth for 5G front-ends. *Journal of Microelectromechanical Systems* 28(4):575–577. <https://doi.org/10.1109/JMEMS.2019.2922935>
67. Plessky V, Yandrapalli S, Turner PJ et al (2019) 5 GHz laterally-excited bulk-wave resonators (xbars) based on thin platelets of lithium niobate. *Electronics Letters*. 55(2):98–100. <https://doi.org/10.1049/el.2018.7297>
68. Jin H, Liu FM, Xu P et al (2014) On-chip generation and manipulation of entangled photons based on reconfigurable lithium-niobate waveguide circuits. *Phys Rev Lett* 113(10):103601. <https://doi.org/10.1103/PhysRevLett.113.103601>
69. Cheng X, Sarihan MC, Chang K-C et al (2019) Design of spontaneous parametric down-conversion in integrated hybrid sixny-ppln waveguides. *Opt Express* 27(21):30773–30787. <https://doi.org/10.1364/OE.27.030773>
70. Sayem AA, Cheng R, Wang S et al (2020) Lithium-niobate-on-insulator waveguide-integrated superconducting nanowire single-photon detectors. *Appl Phys Lett* 116(15):151102. <https://doi.org/10.1063/1.5142852>
71. Dutta S, Zhao Y, Saha U et al (2023) An atomic frequency comb memory in rare-earth-doped thin-film lithium niobate. *ACS Photonics* 10(4):1104–1109. <https://doi.org/10.1021/acsp Photonics.2c01835>
72. Zhang M, Buscaino B, Wang C et al (2019) Broadband electro-optic frequency comb generation in a lithium niobate microring resonator. *Nature* 568(7752):373–377. <https://doi.org/10.1038/s41586-019-1008-7>
73. Ma Z, Chen J-Y, Li Z et al (2020) Ultrabright quantum photon sources on chip. *Phys Rev Lett* 125(26):263602. <https://doi.org/10.1103/PhysRevLett.125.263602>
74. Snigirev V, Riedhauser A, Lihachev G et al (2023) Ultrafast tunable lasers using lithium niobate integrated photonics. *Nature* 615(7952):411–417. <https://doi.org/10.1038/s41586-023-05724-2>

Publisher's Note Springer Nature remains neutral with regard to jurisdictional claims in published maps and institutional affiliations.



Yixin Zhu received his Master's Degree in Physics from Qingdao University in 2017. He is currently a PhD candidate at the School of Electronic Science and Engineering, Nanjing University, Nanjing, China. His research interests include neuromorphic devices and applications.



Qing Wan Director of the Yongjiang Laboratory Heterogeneous Integration Research Center. He obtained his undergraduate degree in the Department of Materials at Zhejiang University and earned a Ph.D. in Microelectronics from the Shanghai Institute of Microsystem and Information Technology, Chinese Academy of Sciences in 2004. After completing his Ph.D., he conducted postdoctoral and visiting professor research at the University of Cambridge, the University of Michigan, and Stanford University. Upon returning to China, he held positions at Hunan University, the Ningbo Institute of Materials Technology, Chinese Academy of Sciences, and Nanjing University. In 2014, he was supported by the National Science Fund for Distinguished Young Scholars. Currently, his primary research activities are carried out at the Yongjiang Laboratory.